Computer Simulation of Ribonuclease Action on Uridylyl-(3′–5′)-adenosine[1]

Robert R. Holmes,* Joan A. Deiters, and Judith C. Gallucci[2]

*Contribution from the Department of Chemistry, University of Massachusetts,
Amherst, Massachusetts 01003. Received April 12, 1978*

Abstract: The first step of the hydrolytic action of ribonuclease on the dinucleotide substrate UpA is investigated via molecular mechanics calculations. UpA coordinates were obtained by conformational minimization of the UpcA coordinates from the X-ray diffraction study of RNase-S with UpcA. Only the amino acid residues in the immediate vicinity of the active site were included in the calculations: histidine-12, histidine-119, and lysine-41. It is found that histidine-119 and lysine-41 may be moved into more favorable positions for contact with the phosphate group with little change in energy. The transphosphorylation step is initiated by decreasing the $O_{2'}$ to phosphorus distance while simultaneously increasing the $O_{5'}$ to phosphorus distance, resulting in cleavage of the P–$O_{5'}$ bond and formation of the 2′,3′-cyclic intermediate. The phosphorus atom moves almost 2 Å in forming this cyclic intermediate, bringing the phosphate unit within the hydrogen-bonding distance of lysine-41. Distances between the dinucleotide and the amino acid residues in both the initial structure and the cyclic intermediate support a proposed reaction mechanism involving hydrogen bonding. The reaction proceeds by an in-line attack of the $O_{2'}$ oxygen atom on phosphorus and passes through a transition state which lies along the Berry coordinate. The transition-state structure is determined to be intermediate in geometry between a trigonal bipyramid and a square pyramid. Compatible with the enzyme catalysis, the computed ground state, transition state, and cyclic intermediate structures have comparable energies.

Introduction

Two powerful approaches to the understanding of enzyme mechanisms involve the use of paramagnetic probes in determining active-site geometries via NMR[3] and single-crystal X-ray diffraction studies.[4] In either of these methods, the use of transition-state analogues aids in the mechanistic interpretation. Computer modeling of enzyme–substrate complexes provides a third approach which has received increased attention.[5] However, because of the lack of sufficient background data, either on the enzyme active-site region or on possible transition-state conformations, no complete structural delineation of a mechanistic sequence has appeared.

A great deal of experimental work has been done on the enzyme ribonuclease A, which catalyzes ribonucleic acid cleavage.[6,7] The hydrolysis mechanism consists of two steps as shown in Figure 1: (1) the phosphodiester bond is cleaved and a 2′,3′-cyclic nucleotide is formed along with a free 5′-OH group; (2) the cyclic nucleotide is hydrolyzed to form a 3′-nucleoside monophosphate.

Although the details of these steps are interpreted in many ways, several points are generally accepted:[6] (1) phosphorus is attacked by a nucleophilic oxygen atom as a result of catalysis by the enzyme; (2) the transition state formed is a pentacoordinate phosphorus structure; (3) the leaving group is catalytically protonated; and (4) at least two out of the three amino acid residues of the enzyme active-site region are important to the reaction, histidine-12, histidine-119, and lysine-41.

This paper deals with the calculation of a reaction pathway for the first step of ribonuclease hydrolysis. The above four points were used as a basis for this work along with the mechanism proposed by Roberts et al.[8] Of particular interest here is the calculation of the possible geometries about phosphorus as it changes from a 3′,5′-phosphodiester linkage, to a five-coordinate transition state, and finally to a cyclized phosphate group.

A molecular mechanics calculation was applied to the first step of the reaction. In general, a molecular mechanics approach to conformational analysis relates the strain energy of a molecule to a specific conformation and, by means of a minimization technique, seeks the conformation of minimum strain energy. We have extended the molecular mechanics program of Allinger et al.[9] for calculations on phosphorus compounds. In a previous paper,[10] the main structural features

of a variety of phosphoranes were reproduced by this molecular mechanics model, parameterized for nonrigid five-coordinate phosphorus.[10]

Pentacoordinate phosphorus belongs to a special class of compounds exhibiting stereochemical nonrigid behavior. It has been established that the structural distortion (imposed by constraints due to the specific ligand arrangement) between the trigonal-bipyramidal and square-pyramidal geometries of phosphoranes is a consequence of low angle bending force constants at phosphorus with the Berry exchange coordinate governing this distortion.[11] In contrast to coordination numbers of two, three, four, and six, added flexibility is available to phosphoranes in achieving a structure of minimum energy. A knowledge of this feature of five-coordinate phosphorus is essential to establishing any conformational scheme.

In application of the molecular mechanics method,[12] the energy for a molecule is calculated as a sum of several potential functions

$$E_{\text{steric}} = \Sigma E_{\text{str}} + \Sigma E_{\text{bend}} + \Sigma E_{\text{tors}} + \Sigma E_{\text{nB}} + \Sigma E_{\text{EPR}} \quad (1)$$

The stretch and bend terms are modified Hooke's law expressions; E_{tors} is the torsional-energy contribution computed by a cosine law; E_{nB} includes van der Waals interactions between atoms not bonded to a common atom; and E_{EPR} is a term for energy of repulsion between atoms bonded directly to phosphorus, due to their electron-pair interactions.[10] It was necessary to introduce this last term to obtain good agreement between calculated and experimentally determined structures for the phosphoranes.[10] For each term, the sum is over all interactions for the molecule and the total energy is minimized with respect to all positional coordinates.

Initial Enzyme–Substrate Coordinates (ESC Set) for UpA. Richards and Wyckoff[13] have published the coordinates for the substrate analogue UpcA in the enzyme ribonuclease S resulting from an X-ray study at 2-Å resolution. RNase-S is a catalytically active form of RNase-A, where a bond in the vicinity of residues 19–22 has been cleaved. UpcA is an altered dinucleotide which corresponds in all respects to the usual dinucleoside phosphate UpA [uridylyl-(3′-5′)-adenosine] except that the 5′-oxygen atom of the ribose attached to the adenine base has been replaced with a methylene group. The P–C bond thus present is not cleaved by ribonuclease in the X-ray study.

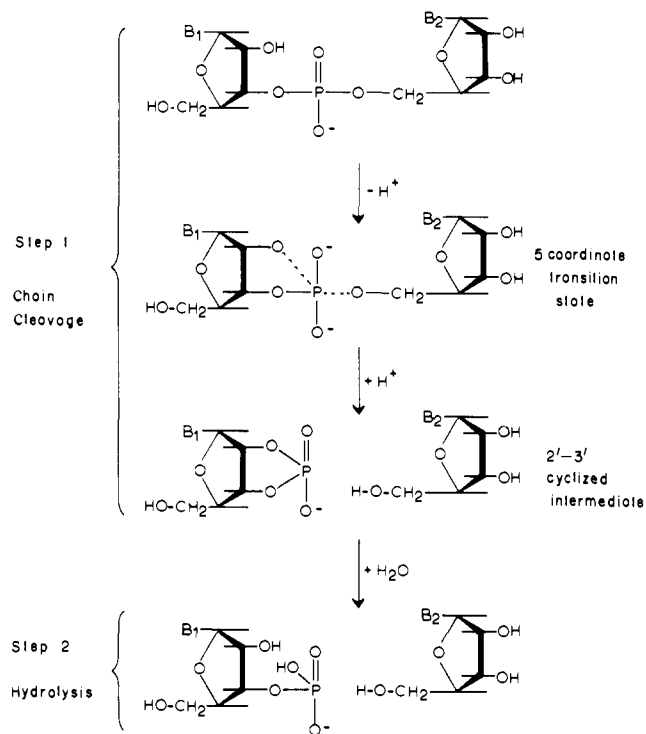In establishing a set of coordinates for the enzyme–substrate

Figure 1. The transphosphorylation and hydrolysis steps of ribonuclease action on a dinucleotide substrate.

Figure 2. Numbering scheme used for the enzyme-substrate system RNase-UpcA.

complex, the UpcA results (list II of ref 13) were used as starting coordinates in the energy minimization calculation with the CH_2 group being replaced by an oxygen atom. The molecular mechanics program by Allinger et al.,[9] modified as mentioned in the introduction for pentacoordinate phosphorus,[10] formed the basis for the computer minimization.

Figure 2 shows the numbering scheme used for the calculation. Our model for this system includes UpA as the substrate analogue with histidine-12, histidine-119, and lysine-41 positioned in the active site. Only these three important amino acid residues were used, to keep the system relatively small for computational purposes. However, we note that recent work by Walter and Wold[14] suggests that lysines-7 and -66 may substitute for the role assigned to lysine-41.

This unconventional numbering scheme was used so that each atom, whether in the enzyme or substrate, is designated by a single number. Atoms 54 and 55 are oxygen atoms of water molecules found at the active site in the UpcA X-ray study.[13] The conventional numbering scheme for UpA is given in Figure 3. Both sets of numbers are used in Table V, to be discussed later.

Model Parameterization. In the molecular mechanics calculations, the sources of the values for "strainless" bond lengths, bond angles, and van der Waals parameters were Allinger's programmed values,[9] values from an X-ray study of Sussman and Seeman[15] of the structure of crystalline UpA, and parameters from our earlier work on the conformational minimization of phosphoranes.[10] When force constants were required for variations in P-O bond lengths, Badger's rule was applied.[16]

Torsional constants were used only for the uracil, adenine, and imidazole planes. The latter bases were held in a planar configuration by assigning a sufficiently high value to the appropriate torsional constants. All bending force constants for angles at phosphorus (X-P-Y) were set to zero, in keeping with the findings in our earlier study on the stereochemical nonrigidity associated with pentacoordinate phosphorus.[10] As a result, the phosphate group is not constrained to a particular
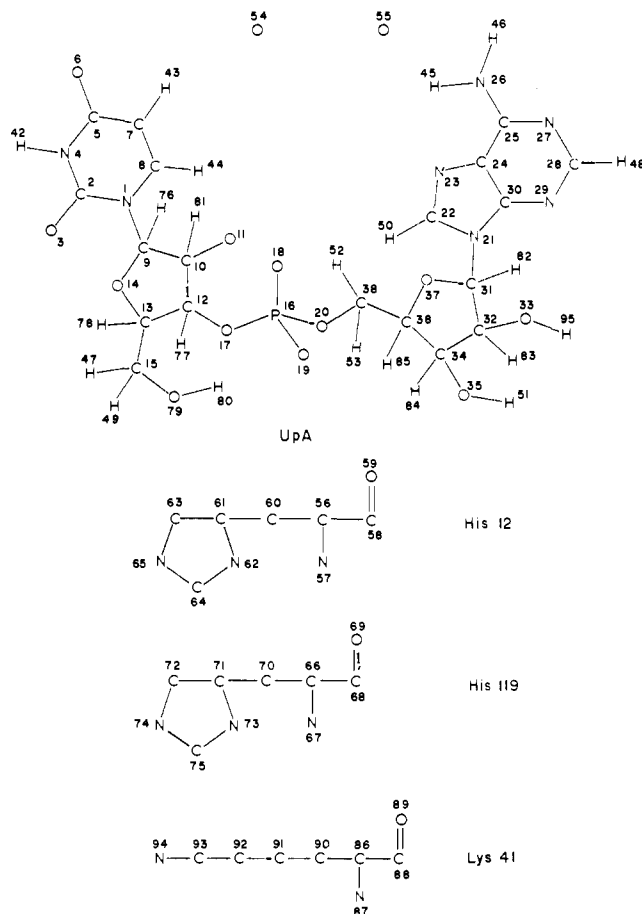
geometry, during minimization, by the imposition of sets of "strainless" angles for the trigonal-bipyramidal or square-pyramidal idealized conformations. Also the angles $C_{12}O_{17}P$, $C_{38}O_{20}P$, and $C_{10}O_{11}P$ were given a zero bending force constant to allow them freedom to change values during the cyclization step.

Because of the limitations of the X-ray resolution of 2 Å in the ribonuclease S study with UpcA in place, the UpcA coordinates of the individual atoms of list II of ref 13 represent a certain amount of strain energy by our calculation. An initial energy of 316.2 kcal/mol was calculated for these X-ray coordinates. The distribution of this initial strain energy (Table I, column 1) is centered in the bond-stretching and -bending terms. Some of the bond lengths of UpcA in the enzyme X-ray study differ by about 0.1 Å from those determined from high-resolution X-ray studies that are possible on the individual bases and ribose moieties. For example, the $C_{12}-C_{13}$ bond length calculated from the UpcA enzyme substrate[13] is 1.42 Å while the same bond in native UpA[15] is 1.53 Å.

Minimum Energy Conformation of RNase-UpcA and RNase-UpA. In order to obtain UpcA and UpA structures of lower strain energy, the substrate atoms were moved slightly from their initial X-ray positions. However, the positions of the adenine and uracil base planes were maintained the same as in the X-ray results, as it is thought that these positions may be due to enzyme constraints.

In general, for this and subsequent calculations, the water molecules were held fixed unless otherwise noted. The histidine carbonyl carbon atoms were held fixed and the imidazole planes were held in their X-ray positions unless specific rotations are described. The movement of histidine-119 toward the phosphate group was performed and will be discussed in a
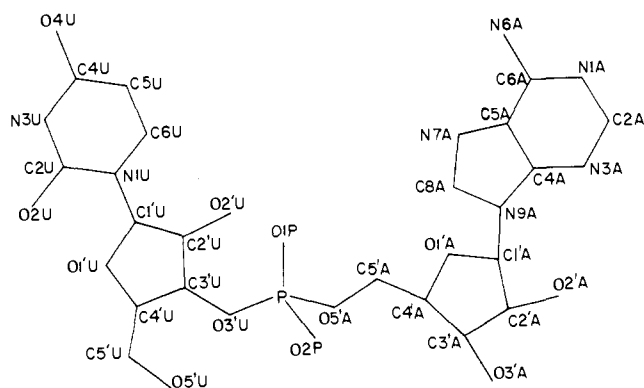
Figure 3. Conventional numbering scheme for UpcA.

Table I. Steric Energy (kcal/mol) for X-ray Coordinates of Enzyme-Bound UpcA, Conformationally Minimized UpcA, and UpA

energy	UpcA[a] (X-ray)	UpcA[b]	UpA[b] (ESC-A)	UpA[b] (ESC-B)
bond stretch	267.49	1.31	1.04	0.95
bond bend	41.43	6.85	7.08	5.95
VDW	−5.47	−6.65	−5.74	−5.13
EPR	7.06	6.29	3.93	4.05
torsion	5.71	0.68	0.77	0.70
torsion bend	−0.01	0.00	0.00	0.00
total energy	316.22	8.48	7.08	6.53

[a] Initial energy calculated from X-ray coordinates (list 11, ref 13) of UpcA substrate in ribonuclease S and those of histidine-12, histidine-119, and lysine-41. The contribution of O_{79} and of all hydrogen atoms was not included since no coordinates were available. [b] UpcA, UpA (ESC-A), and UpA (ESC-B) are calculated minimum energy conformations. The contribution of O_{79} and of all hydrogen atoms is included. The sets differ in that UpcA has a carbon atom at position 20 which is replaced by oxygen in the UpA calculations. In ESC-B, histidine-119 is rotated 60°C from its position in ESC-A. [c] In the calculation of the electron pair repulsions term (EPR), a D value of 0.1 was used. See ref 10 for the origin of this term.

following section. For lysine-41, the carbonyl carbon and the ε-carbon atom were held fixed and the remainder of the chain was "free" to move in all minimizations.

The end result is an adjusted set of coordinates for UpcA and UpA (ESC-A). (See columns 2 and 3, Table I, for the strain-energy distribution.) Another coordinate set for enzyme-bound UpA (ESC-B) is described later in the text.

Figure 4 displays an ORTEP drawing of the minimum-energy coordinates for enzyme-bound UpA (ESC-A) superimposed on the X-ray coordinates of Richards and Wyckoff[13] for UpcA (lighter lines). Hydrogen atoms are omitted for clarity; however, they were included in the energy minimization. The principal difference between these two structures lies in the position of the phosphate moiety.

Significant structural features of the X-ray coordinates for UpcA, those for the minimum energy set for UpA, and the crystal coordinates for UpA obtained by Sussman and Seeman[15] are compared in Table II. The relative orientation of the enzyme-bound base planes differs considerably from that in the native UpA crystal. The enzyme constraints produce an appreciable shortening of the important $P-O_{11}$ nonbonded distance in UpcA compared to that in native UpA. This shortening is also evident in the computed enzyme-bound UpA minimum-energy structure. Since this ribose oxygen O_{11} attacks phosphorus in the first step of RNase action, shortening of the $P-O_{11}$ distance from its value of 4.11 Å in native UpA
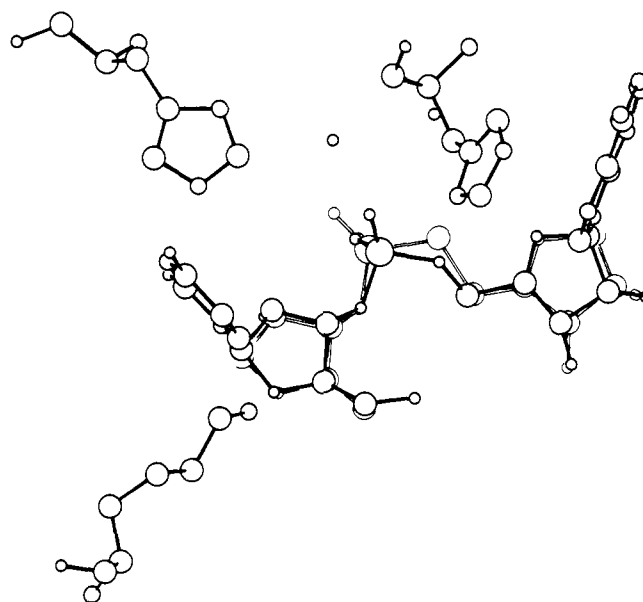

Figure 4. ORTEP drawing of the minimum energy structure for enzyme-bound UpA (ESC-A) superimposed on the X-ray coordinates of UpcA that show significant differences (lighter lines).

Table II. Some Structural Parameters for Enzyme-Bound UpcA and UpA and for Native UpA

	enzyme bound			native
	UpcA,[a] X-ray	UpcA,[b] computed	UpA[b](ESC-A) computed	UpA,[c] X-ray
Bond Lengths, Å				
$P-O_{17}$	1.61	1.61	1.61	1.62
$P-O_{18}$	1.46	1.46	1.48	1.47
$P-O_{19}$	1.66	1.65	1.47	1.48
$P-C_{20}$	1.85	1.85		
$P-O_{20}$			1.61	1.60
Bond Angles, Degrees				
$O_{17}-P-O_{18}$	113.1	105.4	107.1	108.9
$O_{17}-P-O_{19}$	110.1	102.9	112.2	110.0
$O_{17}-P-C_{20}$	106.0	108.9		
$O_{17}P-O_{20}$			102.0	100.6
$O_{18}-P-O_{19}$	108.3	104.7	111.9	118.8
$O_{18}-P-C_{20}$	106.0	120.0		
$O_{18}-P-O_{20}$			110.2	106.6
$O_{19}-P-C_{20}$	113.4	113.4		
$O_{19}-P-O_{20}$			112.9	110.7
Nonbonded Distance, Å				
$P-O_{11}$	3.31	3.53	3.51	4.11[d]
Dihedral Angles, Degrees				
(1) uracil–adenine[f]	64.5	64.6	64.6	11[e]
(2) imidazole ring of His-12 and His-119[f]	65.9	65.9	65.9	

[a] Coordinates from ref 13. [b] From minimum-energy coordinate set as discussed in text; $D = 0.1$. [c] From ref 15. There are two different molecules of UpA per asymmetric unit. Distances and angles listed have been calculated from the positional parameters reported for UpA2. The corresponding values for UpA1 are only slightly different from those for UpA2. [d] In UpA1, the $P-O_{11}$ distance is 3.81 Å. [e] In UpA1, the dihedral angle between the uracil and adenine base planes is 18°. [f] Planes.

to 3.5 Å in enzyme-bound UpA would facilitate nucleophilic attack.

The angle sets shown in columns 1 and 2 (Table II) differ somewhat from each other. Since the bending force constants

Table III. Sugar Ring Puckering Observed in Calculated and X-ray UpcA and UpA Structures[a]

	enzyme bound				native
	UpcA, X-ray	UpcA, computed	UpA (ESC-A), computed	UpA (ESC-B), computed	UpA, X-ray
Distances from Reference Plane Formed by $C_{4'U}$–$O_{1'U}$–$C_{1'U}$, Å					
$C_{2'U}$	−0.110	−0.136	0.095	−0.247	0.270
$C_{3'U}$	−0.473	−0.458	−0.465	−0.601	−0.335
$C_{5'U}$	−0.559	−0.896	−0.886	−0.782	−0.884
Distances from Reference Plane Formed by $C_{4'A}$–$O_{1'A}$–$C_{1'A}$, Å					
$C_{2'A}$	−0.090	−0.279	0.366	0.142	−0.113
$C_{3'A}$	0.636	0.072	0.764	0.504	0.437
$C_{5'A}$	0.902	1.166	0.585	0.872	0.912

[a] The conventional numbering scheme of Figure 3 is used here.

Table IV. Distances between Key Atoms[a] in RNase-UpA Complex (ESC-A and ESC-B Sets)

key atoms		distance, Å	
		ESC-A	ESC-B[b]
N_{65}–O_{11}	(N_{65} of histidine-12)	3.85	3.56
N_{73}–O_{20}	(N_{73} of histidine-119)	3.82	3.05
N_{73}–O_{19}		3.15	2.98
N_{94}–O_{18}	(N_{94} of lysine-41)	7.44	5.84
O_{54}–O_{18}		2.95	4.28
O_{54}–O_{19}	(O_{54} of a water molecule)	4.24	3.17
P–O_{11}		3.51	3.21

[a] Atom numbering is that found in Figure 2. [b] Same as ESC-A, except for a rotation of histidine-119 by 60° about the C_{66}–C_{70} bond as described in the text.

for all phosphorus angles were given zero values, there was nothing in the calculation which constrained these angles to values shown in column 1 for the X-ray structure. Slight adjustments in atomic coordinates from UpcA (X-ray) to UpcA (computed) as we have performed can give rise to these angle disparities. In comparing the computed angles for UpcA to those for UpA (columns 2 and 3, Table II), several differences are noted due to the substitution of O_{20} for the CH_2 group. The presence of the CH_2 group causes the angles involving C_{20} to open compared to the O_{20} angles.

With reference to the atom labeling in Figure 3, the kinds of puckering observed in the ribose units of each nucleotide are tabulated in Table III. The method suggested by Arnott[17] is used, where $C_{1'}$–$O_{1'}$–$C_{4'}$ form a reference plane and the distances of $C_{2'}$, $C_{3'}$, and $C_{5'}$ from this plane are calculated. For the ribose ring bonded to uracil, both the UpcA X-ray and calculated structures show an unusual mode of puckering, i.e., the $C_{2'U}$ and $C_{3'U}$ are on the same side of the reference plane. The fact that the puckering does not change much between these two structures shows that the calculations do not impose unreasonable constraints upon the sugar ring conformation. In the UpA ESC-A structure, the $C_{2'U}$ has moved to the other side of the reference plane, resulting in a 3'-endo conformation, which is also found in the native UpA X-ray structure. Upon histidine-119 movement, the UpA ESC-B model reverts again to the unusual puckering mentioned above. Both glycosidic bonds in all structures have the anti conformation.

In summary, we have used the UpcA coordinates from an X-ray study to obtain minimum-energy structures for UpcA and UpA in the active site of RNase-S. The resulting structure for UpA will now be examined relative to the possible reaction pathways encountered in the first step of the enzyme reaction.

Reaction Mechanism. In a proposed mechanism of ribonuclease action on RNA proceeding via a pentacoordinate transition state, Roberts et al.[8] discuss the roles of histidine-12, histidine-119, and lysine-41. With reference to the atom numbering in Figure 2, these important mechanistic features are summarized here. A nitrogen atom of histidine-12, within hydrogen-bonding distance of O_{11}, facilitates phosphorus attack by O_{11} by proton withdrawal. A nitrogen atom of histidine-119 is close enough for hydrogen bonding to a phosphoryl oxygen O_{19} and to the phosphoester oxygen O_{20} for protonation to occur upon cleavage of the P–O_{20} bond (i.e., the 5'-ester bond in the accepted nomenclature). Lysine-41 is also indicated by Roberts et al.[8] to form a hydrogen bond to a phosphoryl oxygen in the enzyme–substrate complex, although Richards and Wyckoff[13] suggest that this hydrogen bonding is possible only after cyclization has taken place. Cyclization is proposed to take place in-line, i.e., apical approach of O_{11} and apical departure of O_{20}, in a trigonal-bipyramidal transition state.

The second step is essentially the reverse of the first, where a water molecule which is near O_{18} and O_{19} takes the place of O_{11} (2'-oxygen). The resulting ring opening gives a terminal nucleoside 3'-phosphate.

It has been suggested that the cyclization reaction may proceed through an in-line square-pyramidal transition state.[18] The three amino acid residues play the same role in the latter proposal as they do in Roberts' proposal. In fact, the positions of histidine-119 and lysine-41 residues are believed to be rather labile.[19] As a result, they were moved into positions more favorable for interaction with the phosphate group. These movements are described in the following sections.

We have examined our ground-state structure for UpA with respect to distances between the phosphate group and the amino acid residues. The results are given in Table IV. Note that the distances between the imidazole nitrogens and phosphate oxygens look fair for possible hydrogen bonding in ESC-A. In ESC-B, these distances have been decreased by moving the imidazole ring of histidine-119 closer to the phosphate group. Since a molecular model of ribonuclease S shows considerable freedom for histidine-119 rotation about the C_{66}–C_{70} bond, we calculated minimum-energy conformations for the ESC-A coordinates as a function of rotation about this bond. It was found that a 60° rotation of the imidazole ring (counterclockwise when viewed along the C_{66}–C_{70} bond with C_{70} closest to the viewer) not only decreases the nitrogen to oxygen distances but also results in shortening the P⋯O_{11} distance by 0.3 Å. Together with the increase in the O_{11}–P–O_{20} angle from 141° in ESC-A to 154° in ESC-B (not shown in Table IV), these results favor an in-line attack of the O_{11} on the phosphate group. The energies for ESC-B are listed in Table I, column 4. In both ESC-A and ESC-B, the oxygen atom O_{54} of one of the two water molecules found in the enzyme active-site region is close enough to O_{18} and O_{19} to participate in the second step of the reaction.

A similar calculation was done by Lipkind and Karpeiskii[20] to determine the effect of movement of histidine-119. They found that the most probable value for the C_α–C_β torsion angle (N_{67}–C_{66}–C_{70}–C_{71}) was ∼80°, while the C_β–C_γ torsion angle ($C_{66}C_{70}C_{71}$–N_{73}) has a wide range of values. In our results ESC-A has a C_α–C_β angle of 79° with C_β–C_γ equal to 130°, while ESC-B has a C_α–C_β angle of 153° and a C_β–C_γ of 120°. Compared to ESC-A, ESC-B has the histidine-119 rotated into a better position for interaction with the phosphate group of UpA. Lipkind and Karpeiskii found their best position for histidine-119 by moving it into a location suitable for hydrogen bonding with the nearby amino acid residue of asparagine-121. They later included U > p in the calculations, but left out the adenosine portion, which may have an effect on the histidine-119 position.

Lastly, the distance of the terminal nitrogen atom of lysine-41 to a phosphoryl oxygen (N_{94}⋯O_{18}) is too large for ef-

fective interaction in the enzyme-substrate complex. Later, we show that after cyclization has occurred with the accompanying phosphorus movement, it is possible for lysine-41 to move easily into a position for effective interaction with O_{18}. However, before cyclization, an attempt to decrease the $N_{94}\cdots O_{18}$ distance to 3.8 Å or less resulted in a large increase of strain energy in the angles of the lysine chain, whereas this was not the case after cyclization.

In summary, the geometry for UpA in the active site of RNase-S that has been calculated by our molecular mechanics method (ESC-B) conforms to the mechanism proposed by Roberts et al.[8] in regard to hydrogen-bonding distances between the phosphate group and the amino acid residues. This structure appears suitable for use as an enzyme-substrate complex and for use in constructing a cyclic intermediate for the first step of the reaction.

Cyclized Intermediate. In the first step of the ribonuclease reaction, i.e., the cyclization step, the $P-O_{20}$ bond is broken and a new bond $P-O_{11}$ is formed to give a four-coordinate phosphorus cyclic intermediate. In order to obtain an intermediate via computer modeling, an energy minimization was carried out in the following way. Initial coordinates for the enzyme-bound substrate system (ESC-B) were reminimized into a cyclic intermediate (CI) conformation by changing two "strainless" bond lengths (i.e., $P-O_{11}$ was decreased from 3.5 to 1.60 Å while $P-O_{20}$ was increased from 1.60 to 3.5 Å) and holding all other bond parameters at the values used for ESC minimization. The force constants for these two bonds were changed accordingly. The uracil and adenine planes, the two water molecules, the carbonyl carbons of the three amino acid residues, the ϵ carbon of lysine-41, and the imidazole planes of histidine-12 and -119 were held fixed in position while all the other atoms of the system were free to move into the minimum-energy conformation of the cyclized intermediate.

An ORTEP drawing of the resulting structure is shown in Figure 5. Bond distances and angles are tabulated in column 1 of Table V. The strain energy of the cyclic intermediate (6.12 kcal/mol) is quite comparable to the energy of the uncyclized dinucleotide, ESC-B (6.53 kcal/mol). In forming this cyclic intermediate, phosphorus moves about 1.85 Å from its original position at the active site, in good agreement with the prediction of Richards and Wyckoff[21] that a phosphorus motion of approximately 2 Å is needed to form a cyclic intermediate.

An X-ray diffraction study by Coulter[19] of sodium β-cytidine 2',3'-cyclic phosphate provides a structure for comparison to the minimum-energy, cyclized intermediate. Values from Coulter's study are shown in columns 3 and 4 of Table V. The cytosine base in the X-ray study is in the syn conformation while the uracil base in our calculation is in the anti conformation. Internal ring angles and torsional angles from the X-ray study appear to differ considerably from our calculated cyclic intermediate structure, CI-A, but if we introduce some additional constraints, it is possible to get a minimum-energy, cyclized intermediate which has bond distances and angles similar to Coulter's. The additional constraints are nonzero force constants for three bond angles ($P-O_{11}-C_{10}$, $P-O_{17}-C_{12}$, and $O_{11}-P-O_{17}$) and a nonzero torsional constant, V_2, for the torsional angle $O_{11}C_{10}C_{12}O_{17}$. The strain energy for this cyclic intermediate (CI-B) is similar to that of cyclic intermediate A. Parameters for CI-B are tabulated in column 2 of Table V.

We conclude that both calculated cyclic structures are reasonable models for intermediates in the action of ribonuclease on the dinucleotide UpA. Although the CI-B structure more closely resembled the X-ray structure of native 2',3'-cyclic cytosine, we preferred to use the CI-A structure for further calculations, because it had no angle bending force constant constraints on the angles at phosphorus. Since we had imposed no phosphorus bending force constants on the original
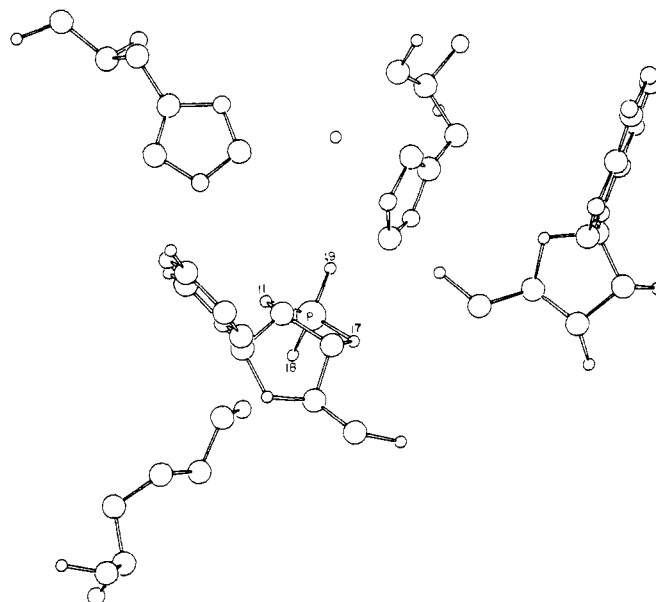

Figure 5. ORTEP drawing of the minimum energy conformation of the 2',3'-cyclic intermediate (CI-A) in the UpA-RNase system. The atom numbering is from Figure 2. For comparison with the more conventional atom numbering in Figure 3, $C_{10} = C_{2'U}$; $C_{12} = C_{3'U}$; $O_{11} = O_{2'U}$; $O_{17} = O_{3'U}$.

UpA conformation, and wished to impose none on the five-coordinate transition state, we chose the cyclic intermediate CI-A. Also it is reasonable to expect some structural variation within the cyclic moiety on going from the native crystal to the enzyme environment.

Lysine Movement. As previously mentioned, the terminal nitrogen of lysine-41 is possibly important in hydrogen bonding to phosphoryl oxygens. The $N_{94}-O_{18}$ distance in the dinucleotide coordinate set ESC-B is 5.8 Å, and in the cyclic intermediate CI-A the same parameter is 4.8 Å. Neither distance is short enough for effective hydrogen bonding. In order to see if lysine-41 could be brought within hydrogen-bonding distance with no increase in strain energy, a series of calculations was carried out on the enzyme substrate ESC-B and the cyclized intermediate (CI-A) coordinates.

In this series, N_{94}, the terminal nitrogen of lysine-41, was held by a strong pseudobond to the nearest phosphoryl oxygen O_{18}. This was done by using a large force constant of 25 mdyn/Å for this bond. The calculations were performed for various l_0 values for this bond which varied from 2.6 to 3.6 Å, in increments of 0.2 Å. Only the atoms of the lysine chain were free to move. The carbonyl carbon of lysine and all the other atoms in the system were fixed in position. Thus, in order for a particular l_0 value to be attained for the $N_{94}-O_{18}$ "bond", the lysine chain would have to undergo either rotation about torsional angles, translation of the chain, bond stretching, or bond bending. If only rotation about torsional angles or translation occurs, then the lysine can easily approach the O_{18} atom with no increase in strain energy for the system. But if bond stretching or angle bending occurs to any great extent, the system will be more strained and the corresponding l_0 value cannot easily be attained.

Steric energies for each minimized structure are shown in Table VI. In the dinucleotide-enzyme complex, the strain energy increases as soon as the $N_{94}\cdots O_{18}$ distance decreases to 3.6 Å. It continues to increase at a faster rate as the "bond" length gets smaller. The increase in energy is due to distortion in the C–C–C bond angles and stretching of the C–C bonds of the lysine chain. With the cyclic intermediate structure, lysine-41 can easily be brought within hydrogen-bonding

Table V. Structural Parameters of 2′,3′-Cyclic Phosphates[a]

	UMP (calcd) enzyme-substrate complex		CMP (X-ray[d]) native crystal, sodium salt	
	CI-A[b]	CI-B[c]	anion A	anion B
Bond Distances, Å (P-O-C-C-O Cycle)				
P-O$_{11}$ (P-O$_{2'}$)	1.61	1.61	1.62	1.61
P-O$_{17}$ (P-O$_{3'}$)	1.61	1.61	1.61	1.62
C$_{12}$-O$_{17}$ (C$_{3'}$-O$_{3'}$)	1.43	1.43	1.47	1.46
C$_{10}$-C$_{12}$ (C$_{2'}$-C$_{3'}$)	1.54	1.54	1.54	1.57
C$_{10}$-O$_{11}$ (C$_{2'}$-O$_{2'}$)	1.43	1.43	1.47	1.46
Additional Phosphorus Bond Distances, Å				
P-O$_{18}$ (P-O$_1$)	1.48	1.48	1.47	1.47
P-O$_{19}$ (P-O$_2$)	1.48	1.47	1.48	1.49
Internal Ring Angles in P-O-C-C-O Cycle, Degrees				
O$_{11}$-P-O$_{17}$ (O$_{2'}$-P-O$_{3'}$)	103.0	98.0	96.0	95.7
P-O$_{17}$-C$_{12}$ (P-O$_{3'}$-C$_{3'}$)	107.9	111.9	111.6	111.0
O$_{17}$-C$_{12}$-C$_{10}$ (O$_{3'}$-C$_{3'}$-C$_{2'}$)	109.7	108.0	106.5	106.7
C$_{12}$-C$_{10}$-O$_{11}$ (C$_{3'}$-C$_{2'}$-O$_{2'}$)	108.9	108.0	107.2	106.0
C$_{10}$-O$_{11}$-P (C$_{2'}$-O$_{2'}$-P)	108.5	112.1	112.1	112.2
Additional Phosphorus Bond Angles, Degrees				
O$_{11}$-P-O$_{18}$ (O$_{2'}$-P-O$_1$)	109.6	110.4	110.2	111.1
O$_{11}$-P-O$_{19}$ (O$_{2'}$-P-O$_2$)	108.2	110.2	109.7	111.6
O$_{17}$-P-O$_{18}$ (O$_{3'}$-P-O$_1$)	109.1	110.5	110.4	110.1
O$_{17}$-P-O$_{19}$ (O$_{3'}$-P-O$_2$)	111.8	111.2	109.8	108.9
O$_{18}$-P-O$_{19}$ (O$_1$-P-O$_2$)	114.5	115.2	118.2	117.3
Torsional Angles, Degrees				
H$_{77}$-C$_{12}$-C$_{10}$-H$_{81}$ (H-C$_{3'}$-C$_{2'}$-H)	16.5	4.3	3.6	0.5
O$_{11}$-C$_{10}$-C$_{12}$-O$_{17}$ (O$_{2'}$-C$_{2'}$-C$_{3'}$-O$_{3'}$)	15.3	3.2	6.6	4.0
C$_9$-C$_{10}$-C$_{12}$-C$_{13}$ (C$_{1'}$-C$_{2'}$-C$_{3'}$-C$_{4'}$)	15.1	5.5	5.5	−0.7
P-O$_{17}$-C$_{12}$-C$_{13}$ (P-O$_{3'}$-C$_{3'}$-C$_{4'}$)	102.7	103.1	92.7	95.3
P-O$_{11}$-C$_{10}$-C$_9$ (P-O$_{2'}$-C$_{2'}$-C$_{1'}$)	126.5	110.3	101.5	96.6
Phosphorus Movement from Starting Coordinates (ESC-B), Å	1.85	2.17		
Energy Distribution, kcal/mol				
bond stretch	0.90	0.94		
bond bend	5.64	5.64		
VDW	−4.79	−4.78		
EPR	3.72	3.66		
torsional	0.65	0.73		
total energy	6.12	6.18		

[a] The numbering system refers to numbers used in Figure 2. For convenience the conventional designation (Figure 3) is shown in parentheses. [b] 2′,3′-Cyclic intermediate derived from the enzyme–substrate complex as defined by ESC-B coordinates. [c] Same as CI-A except for changes in four parameters of the calculation as described in text. [d] See ref 19. There are two nucleotide anions per asymmetric unit which differ somewhat from each other in structure.

Table VI. Steric Energies of the Enzyme–Substrate Complex (ESC-B) and of the Cyclized Intermediate (CI-A) as Lysine-41 Approaches the Phosphate Group

N$_{94}$···O$_{18}$ distance, Å	strain energy, kcal/mol	
	ESC-B	CI-A
2.6	17.95	6.02
2.8	13.13	6.06
3.0	10.05	6.07
3.2	8.31	6.09
3.4	7.27	6.10
3.6	6.75	6.12

distance of O$_{18}$ with little distortion in structure and little increase in strain energy.

In both structures, a 3.6-Å distance for N$_{94}$···O$_{18}$ is attainable, but it is more easily reached in the cyclic intermediate than in the ground-state complex. Thus, the role of lysine-41 in binding the dinucleotide at the active site is probably not too important, but, lysine-41 could easily play a role of stabilizing

the cyclic intermediate via hydrogen bonding between its terminal nitrogen N$_{94}$ and the phosphoryl oxygen O$_{18}$.

Pentacoordinate Transition State. The calculated structures for the ground state of UpA and the cyclic intermediate both agree with the proposed mechanism by Roberts et al.[8] for the first step of the reaction with regard to histidine-12, histidine-119, and lysine-41 participation. Hence, it appears that both of these calculated structures are good representatives of the actual systems. Next we consider the possible transition states that may be constructed based on the enzyme-bound ground-state geometry.

Since the majority of the mechanisms proposed for the catalytic activity of RNase[6-8,22,23] involve a pentacoordinate transition state, we wished to simulate a five-coordinate structure by changing the P-O$_{11}$ and P-O$_{20}$ bond parameters. In the calculations, some assumptions were made. Since phosphorus moves 1.9 Å from the unruptured dinucleotide (ESC-B) to the cyclic intermediate (CI-A), the transition state may occur at some point along a straight line between these two phosphorus positions; in the transition state the entering group (O$_{11}$) and the leaving group (O$_{20}$) may form equal bond

Table VII. Steric Energies of Possible Transition States in the RNase-UpA System (kcal/mol)

l_0 values for P-O_{11} and P-O_{20} bonds, Å	phosphorus positions along pathway from ESC-B to C1-A, Å				
		0.50	0.75	1.00	1.25
1.80		17.52	16.28	17.90	22.30
2.00		10.29	9.44	10.89	14.58
2.20		6.65	5.99	7.19	10.21
2.40		5.34	4.80	5.77	8.23
	0.65	0.70	0.75	0.80	0.85
2.10	7.40	7.35	7.36	7.47	7.65
2.15	6.64	6.58	6.60	6.70	6.87

Table VIII. Structural Parameters and Steric Energies of Transition States[a]

	TS-A	TS-B	TS-C
Bond Distances, Å			
P-O_{11}	2.16	2.14	2.13
P-O_{17}	1.61	1.61	1.61
P-O_{18}	1.47	1.47	1.47
P-O_{19}	1.47	1.47	1.47
P-O_{20}	2.16	2.14	2.13
Bond Angles, Degrees			
O_{11}-P-O_{17}	78.8	82.9	91.4
O_{11}-P-O_{18}	104.3	98.6	89.9
O_{11}-P-O_{19}	87.3	89.1	90.0
O_{11}-P-O_{20}	150.2	162.2	179.4
O_{17}-P-O_{18}	112.7	110.1	118.6
O_{17}-P-O_{19}	127.4	133.6	117.4
O_{17}-P-O_{20}	81.6	85.1	88.0
O_{18}-P-O_{19}	119.8	116.3	124.0
O_{18}-P-O_{20}	103.9	97.9	90.3
O_{19}-P-O_{20}	87.1	89.8	90.4
Steric Energy, kcal/mol			
bond stretch	1.68	1.13	0.16
bond bend	6.30	5.91	0.12
VDW	−5.53	−5.34	−0.46
EPR	3.98	3.85	3.64
torsional	0.93	0.83	0.00
total energy	7.35	6.38	3.46

[a] The atom numbering corresponds to that given in Figure 2.

lengths; the strain energy of the transition state should not vary greatly from the energy of the dinucleotide or of the cyclic intermediate. The first two assumptions limit the number of calculations while the third one arises from the conjecture that this fast reaction may be expected to have a low-activation energy.

In the calculation of a minimum-energy structure for a transition state, the same conditions with regard to fixed atoms were used as in the cyclic intermediate calculation, with the following exceptions. Phosphorus was moved along the reaction pathway (i.e., the straight line from its location in ESC-B to its location in CI-A) in increments of 0.25 Å and held fixed at these points during the energy minimization. At each of these phosphorus locations, several possible transition states were calculated by varying l_0 values for the P-O_{11} and P-O_{20} bonds, i.e., the "strainless" bond distance for both the entering and leaving groups. The force constants were varied with bond length as stated earlier. For the equatorial bonds P-O_{17}, P-O_{18}, and P-O_{19}, l_0 was not altered.

The results of this series of calculations are shown in Table VII. For a given phosphorus atom location, as expected, the energy of the transition state decreases as the bond lengths of both the entering and leaving groups increase. For every value of l_0, the strain energy approaches a minimum at a phosphorus
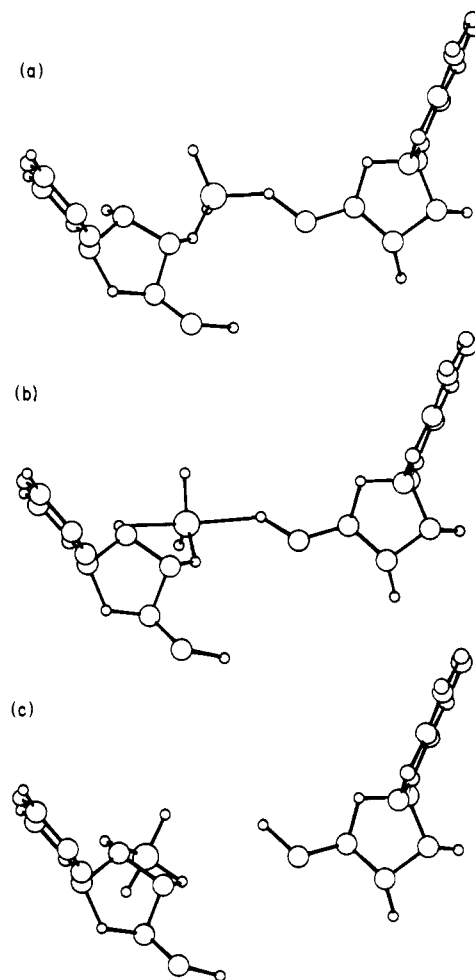

Figure 6. Minimum energy conformations of the dinucleotide UpA in the RNase environment: (a) starting conformation (ESC-B); (b) five-coordinate transition state (TS-A) (axial P-O bonds are 2.1 Å in length); (c) 2',3'-cyclic intermediate (CI-A).

position of 0.75 Å; i.e., when phosphorus has moved approximately 0.75 Å away from its location in the unbroken dinucleotide–enzyme complex, it is in a favorable location for the formation of a five-coordinate transition state where $d_{P-O_{11}}$ = $d_{P-O_{20}}$.

The area about the phosphorus position of 0.75 Å was further investigated, as shown by the last two distance entries in Table VII. At the position of minimum energy, 0.70 Å, both structures have energies similar to the ground-state and cyclic-intermediate energies. We have chosen the result with l_0 = 2.10 Å as being the most feasible transition state. This bond length is close to that reported by Boyd[24] in a molecular orbital calculation on reaction intermediates of cyclic phosphate esters. He estimates a P-O axial distance in a trigonal-bipyramidal transition state in the range 2.2–2.6 Å.

An ORTEP drawing which depicts the phosphorus atom movement as the cyclic intermediate (CI-A) is formed from the enzyme–substrate complex (ESC-B) via the transition state with l_0 = 2.10 Å (TS-A) is shown in Figure 6. Phosphorus bond length, angle parameters, and strain energies are tabulated in Table VIII.

In TS-A, the phosphorus atom was constrained to move along the straight-line path from its position prior to reaction to its position in the cyclized intermediate. Other transition states were calculated without constraint on the phosphorus motion to see if the transition-state geometry would be altered to any great extent. Parameters for one of these calculations are also shown in Table VIII (TS-B). Note that the largest

Table IX. Dihedral Angles, δ, for Transition States and for Ideal Trigonal-Bipyramidal (TP) and Square-Pyramidal (SP) Geometries[a]

edge, δ[b]	TP	TS-C[c]	TS-B[d]	TS-A[e]	SP-1[f]	SP-3[g]
11–19	101.5	102.8	109.2	108.8	118.5	118.5
11–17	101.5	99.0	108.3	108.2	118.5	76.9
19–20	101.5	101.7	109.2	109.1	118.5	118.5
17–20	101.5	99.8	107.7	107.6	118.5	76.9
18–20	101.5	102.5	90.2	89.9	76.9	118.5
11–18	101.5	103.5	88.8	88.6	76.9	118.5
17–18	53.1	53.8	63.0	65.3	76.9	76.9
18–19	53.1	50.8	67.0	71.5	76.9	0
17–19	53.1	54.7	28.2	22.8	0.0	76.9
$\Sigma \|\delta_i(X) - \delta_i(TP)\|$[h]	0.0	13.3	101.1	113.1	217.9	217.9
$\Sigma_i \|\delta_i(X) - \delta_i(SP)\|$	217.9	204.6[i]	116.8[j]	104.8[j]	0.0	0.0
$S - \Sigma_i \|\delta_i(X) - \delta_i(SP)\|$[k]	0.0	13.3	101.1	113.1	217.9	217.9
% motion on Berry coord[l]	0	6	46	52	100	100

[a] All dihedral angles are calculated for unit bond lengths. See ref 11a. [b] Numbering scheme as in Figure 2. [c] Transition state calculated for structure I. It is slightly distorted along the Berry coordinate toward SP-3. [d] Transition state with l_0 (P–O$_{11}$ and P–O$_{20}$) = 2.10 Å. The phosphorus movement is unrestrained. Distortion is along the Berry coordinate toward SP-1. [e] Transition state with l_0 (P–O$_{11}$ and P–O$_{20}$) = 2.10 Å. The phosphorus atom is constrained along a straight line between ESC-B and Cl-A. Distortion is along the Berry coordinate toward SP-1. [f] Square pyramid with atom 18 in apical position. [g] Square pyramid with atom 17 in apical position. [h] X is the transition state, TS-A, TS-B, or TS-C. [i] Calculated from the angles in SP-3. [j] Calculated from the angles in SP-1. [k] S = 217.9. See ref 11a. [l] Percent displacement along the Berry coordinate is given by $[\Sigma_i |\delta_i(X) - \delta_i(TP)|]/S$.

bond angle difference between TS-A and TS-B occurs in the O$_{11}$–P–O$_{20}$ angle, the angle formed by the entering and leaving groups, so that when the phosphorus position is fixed, the resulting transition state is more square pyramidal in character and its energy is slightly higher than when phosphorus is not fixed in position.

**Comparison of "Free" and Enzyme-Bound Transition States.** To see how the dinucleotide–enzyme environment affects the transition-state geometry, we looked at the minimum-energy structure of the isolated fragment I under similar conditions,

I
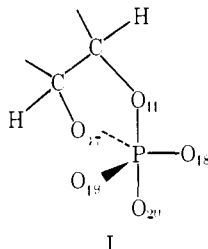
i.e., $l_0(P–O_{11}) = l_0(P–O_{20}) = 2.10$ Å. Structural features of the energy-minimized conformation for I are shown in Table VIII (TS-C). The geometry is quite close to regular trigonal-bipyramidal geometry. The two short phosphoryl bonds, P–O$_{18}$ and P–O$_{19}$, repel each other via the electron-pair repulsion term (EPR), thus causing the equatorial angle to open to 124°. By comparing TS-A and TS-B to this structure, one can see how the dinucleotide–enzyme environment influences the transition state.

For all the transition states calculated, we observed that O$_{11}$ and O$_{20}$ were always positioned in-line [i.e., they occupy axial positions in a trigonal-bipyramidal (TP) geometry or trans-basal positions in a square-pyramidal (SP) form]. The direction and amount of distortion from ideal TP geometry to SP geometry were assessed by the dihedral-angle method.[11a] The results are shown in Table IX.

We calculate the distortion in the dinucleotide–enzyme environment to be along the Berry coordinate, moving toward a square-pyramidal structure with O$_{18}$ as the pivotal atom. The transition-state structure TS-C is only 6% distorted from a
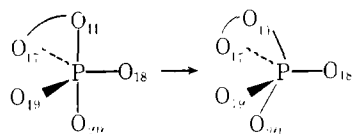
Table X. Steric Energies of Transition States with Angle Constraints for Trigonal-Bipyramidal and Square-Pyramidal Conformations

transition state isomers	steric energy, kcal/mol
TS-B (no force constants used)	6.38[a]
trigonal bipyramids	
O$_{11}$ and O$_{18}$ apical	12.29
O$_{11}$ and O$_{19}$ apical	12.21
O$_{11}$ and O$_{20}$ apical	6.82
O$_{17}$ and O$_{18}$ apical	17.89
O$_{17}$ and O$_{19}$ apical	10.28
O$_{17}$ and O$_{20}$ apical	15.63
square pyramids	
O$_{18}$ apical with O$_{11}$ and O$_{20}$ trans basal	7.03
O$_{19}$ apical with O$_{11}$ and O$_{20}$ trans basal	9.41

[a] From Table VIII.

regular trigonal bipyramid. When the constraints of the enzyme system and the remainder of the UpA molecule are included, the resulting transition states, TS-A and TS-B, are approximately 50% distorted along the Berry coordinate. These results agree with the suggestion of one of the authors[7] that the transition state may be intermediate in geometry between the trigonal-bipyramidal and square-pyramidal forms.

Isomeric Transition States and Pseudorotation. Further calculations on possible transition states were carried out by using TS-B bond lengths and by imposing various bond-angle requirements about the phosphorus atom. These calculations employed the enzyme constraints described for the ground state of UpcA and UpA. Two types of transition states were investigated, trigonal bipyramidal and square pyramidal. In the former, TP angles and bending force constants were imposed on the ten angles having phosphorus as a central atom. The ribose ring always spans apical–equatorial positions. Several TP states were obtained by varying the atoms in the apical positions. In the latter type, SP angles and bending force constants were applied to the ten angles about phosphorus. Only two square pyramids were calculated, one with O$_{18}$ apical and the other with O$_{19}$ apical. Both isomers had the ribose ring spanning cis-basal positions. The results of these calculations are shown in Table X. The sets of angle values, α_0, and force constants, k_b, are those reported in earlier work.[10]
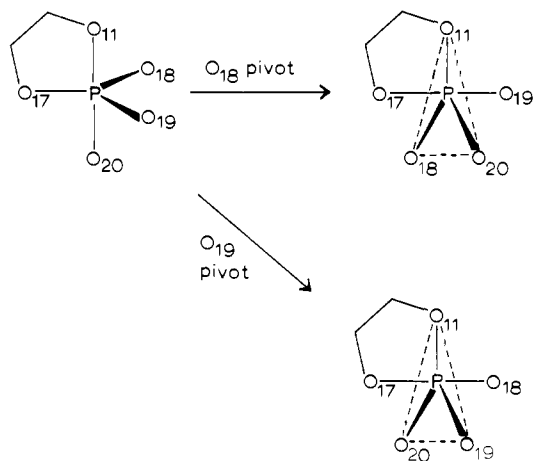
Figure 7. Pseudorotation of the trigonal-bipyramidal transition state formed by an in-line process having O_{11} and O_{20} in apical positions.

Figure 8. Pseudorotation of transition-state trigonal bipyramids formed by adjacent attack.

These results show that the square pyramid with O_{18} apical is of lower energy than that with O_{19} apical and agree with our earlier conclusion that the direction of distortion along the Berry coordinate is toward a square-pyramid structure with O_{18} apical. The TP structure with O_{11} and O_{20} apical is slightly lower in energy than the SP for the dinucleotide-enzyme complex.

A comparison of the six TP isomers shows that the structure with O_{11} and O_{20} in apical positions is of lowest energy, favoring an in-line mechanism. Once this structure is formed, the O_{20} can easily depart from its apical position. If pseudorotation of this intermediate were to occur, the two possible representations shown in Figure 7 would result. By our calculations, these two structures are of much higher energy than the original trigonal bipyramid, so it is unlikely that pseudorotation will occur for an in-line mechanism here. Also, the pseudorotation places O_{20} in an equatorial position, rather than in a leaving apical position.

In considering an adjacent attack where O_{11} enters from an apical position and O_{20}, the leaving group, is in a basal position, there are two possible initial trigonal bipyramids, both of which must pseudorotate to put O_{20} in an apical position for leaving (Figure 8). Both of these isomers with O_{11} and O_{18} apical and O_{11} and O_{19} apical are of high energy. In order for them to pseudorotate, they must go through an even higher energy structure (with O_{17} and O_{20} apical). As a result, the adjacent mechanism seems to be much less favored than the in-line process. And the in-line process with no subsequent pseudorotations is the most energetically favored mechanism by these calculations. It is difficult to say whether the in-line process results in a trigonal bipyramid with O_{11} and O_{20} in apical positions or in a square pyramid with O_{11} and O_{20} in trans-basal positions, since these two structures are of similar energy in our calculations. From the dihedral angle results, a structure intermediate between the two seems most likely.[7]

In summary, our results on transition-state calculations show that a five-coordinate transition state with energy similar to that of the starting coordinates (ESC-B) and of the cyclic intermediate (CI-A) can be simulated. The entering and leaving oxygen atoms occupy apical positions with respect to a TP in a structure intermediate between a regular TP and SP and do not undergo pseudorotation. The direction and degree of the distortion is a result of the geometric constraints of the dinucleotide-enzyme environment as simulated in these calculations.

Reaction-Pathway Barrier Energy. To investigate the reaction pathway in greater detail, we calculated conformation and strain energies along a reaction coordinate at several points
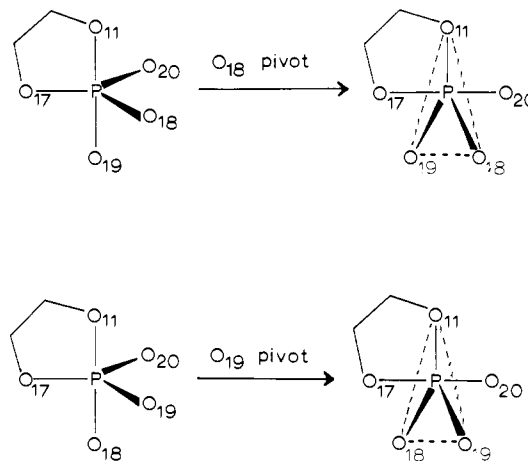
between the ground state and transition state and between the transition state and the cyclic intermediate. From the strain energy at points along this reaction pathway it should be possible to determine if there are high-energy barriers, i.e., structures which forced atoms into close contact with each other or which necessitated large distortions in bond lengths and bond angles as the reaction path was traversed.

Two approaches were used in selecting these points along a pathway for calculation of minimum-energy structures.

(1) The $P-O_{11}$ and $P-O_{20}$ bond lengths were changed in equal increments in going from the ground state to the cyclic intermediate, with the corresponding force constants being determined by Badger's rule.[16]

(2) The force constants for these two bonds were changed in equal increments, with the bond lengths being adjusted accordingly. By either method, the energy at intermediate points does not vary by more than ±1.5 kcal/mol relative to the energy of the initial substrate conformation. It is apparent then that there are no high-energy barriers along either reaction coordinate.

By a slight variation in the relative rate of changing P-O bond lengths, the reaction coordinate can be adjusted to provide a pathway similar in energy to the initial RNase-UpA complex, the transition state, and the cyclized intermediate. From the ORTEP drawing in Figure 6 it is also possible to visualize a movement along a reaction coordinate which does not force atoms into close proximity with one another.

Conclusion

In summary, we have calculated the geometries for UpA constrained at the active site of RNase, for the cyclic intermediate, and for possible transition states between these two points. The histidine-119 and lysine-41 residues were moved into positions more favorable for interaction with the phosphate group. Both the initial enzyme-substrate and the cyclic intermediate support the proposed mechanism of Roberts et al.[8] with respect to hydrogen-bonding distances between the phosphate group and the active-site residues. The most likely transition state arises from an in-line attack and has a five-coordinate structure intermediate in geometry between a trigonal bipyramid and a square pyramid lying along the Berry coordinate. The phosphorus atom moves almost 2 Å upon formation of the cyclic intermediate. In addition, there are no high energy points along a reaction pathway calculated for step one of the RNase reaction.

University of Massachusetts Computing Center for generous allocation of computer time.

Supplementary Material Available: Tables of calculated coordinates for UpcA and UpA (ESC-A, ESC-B, Cl-A, Cl-B, TS-A, TS-B, and the cyclic intermediate with the best lysine-41 position) (8 pages). Ordering information is given on any current masthead page.

References and Notes

(1) (a) Pentacoordinated Molecules. 28. Paper presented in part at the 174th National Meeting of the American Chemical Society, Chicago, Ill., Aug 1977, Abstract No. BIOL 9; (b) for part 27, see R. R. Holmes, *J. Am. Chem. Soc.*, **100**, 433 (1978).
(2) This work represents in part a portion of the Ph.D. thesis of J. C. Gallucci, University of Massachusetts, Amherst, Mass.
(3) (a) A. S. Mildvan, *Acc. Chem. Res.*, **10**, 246 (1977); (b) A. S. Mildvan and M. Cohn, *Adv. Enzymol.*, **33**, 1 (1970).
(4) (a) R. M. Sweet, H. T. Wright, J. Janin, C. H. Chothia, and D. M. Blow, *Biochemistry*, **13**, 4212 (1974); (b) R. Huber, D. Kukla, W. Bode, P. Schwager, K. Bartels, J. Deisenhofer, and W. Steigemann, *J. Mol. Biol.*, **89**, 73 (1974); (c) R. Huber, W. Bode, D. Kukla, U. Kohl, and C. A. Ryan, *Biophys. Struct. Mech.*, **1**, 189 (1975); (d) F. A. Cotton and E. E. Hazen, Jr., "The Enzymes", 3rd ed., Vol. IV, P. D. Boyer, Ed., Academic Press, New York, N.Y., 1971, pp 153–174.
(5) (a) K. E. B. Platzer, F. A. Momany, and H. A. Scheraga, *Int. J. Pept. Protein Res.*, **4**, 187, 201 (1972); (b) G. M. Lipkind and M. Ya. Karpeiskii, *Mol. Biol. (Moscow)*, **10**, 395 (1976); (c) E. M. Popov, *ibid.*, **11**, 5 (1977); (d) I. B. Golovanov, V. M. Sobolev, E. V. Shchukina, and M. V. Vol'kenshtein, *ibid.*, **10**, 7703 (1976).
(6) F. M. Richards and H. W. Wyckoff in ref 4d, Chapter 24, pp 647–806.
(7) See also R. R. Holmes, *Int. J. Pept. Protein Res.*, **8**, 445 (1976), and references cited therein.
(8) G. C. K. Roberts, E. A. Dennis, D. H. Meadows, J. S. Cohen, and O. Jardetzky, *Proc. Natl. Acad. Sci. U.S.A.*, **62**, 1151 (1969).
(9) (a) N. L. Allinger, M. T. Tribble, M. A. Miller, D. H. Wertz, *J. Am. Chem. Soc.*, **93**, 1637 (1971); (b) D. H. Wertz and N. L. Allinger, *Tetrahedron*, **30**, 1579 (1974).
(10) J. A. Deiters, J. C. Gallucci, T. E. Clark, and R. R. Holmes, *J. Am. Chem. Soc.*, **99**, 5461 (1977).
(11) (a) R. R. Holmes and J. A. Deiters, *J. Am. Chem. Soc.*, **99**, 3318 (1977); (b) *J. Chem. Res. (S)*, 92 (1977).
(12) J. E. Williams, P. J. Stang, and P. v. R. Schleyer, *Annu. Rev. Phys. Chem.*, **19**, 531 (1968), have reviewed the calculational methods of conformation analyses.
(13) F. M. Richards and H. W. Wyckoff, "Atlas of Molecular Structures in Biology", Vol. 1, D. C. Phillips and F. M. Richards, Eds., Clarendon Press, Oxford, 1973.
(14) B. Walter and F. Wold, *Biochemistry*, **15**, 304 (1976).
(15) J. L. Sussman and N. C. Seeman, *J. Mol. Biol.*, **66**, 403 (1972).
(16) R. M. Badger, *J. Chem. Phys.*, **2**, 128 (1934).
(17) S. Arnott, *Prog. Biophys. Mol. Biol.*, **21**, 274–275 (1970).
(18) Op. cit. in ref 7.
(19) C. L. Coulter, *J. Am. Chem. Soc.*, **95**, 570 (1973).
(20) G. M. Lipkind and M. Ya. Karpeiskii, *Dokl. Akad. Nauk SSSR*, **224** (No. 5), 1212 (1975).
(21) Op. cit. in ref 6, p 788.
(22) D. A. Usher, D. I. Richardson, Jr., and F. Eckstein, *Nature (London)*, **228**, 663 (1970).
(23) D. A. Usher, E. S. Erenrich, and F. Eckstein, *Proc. Natl. Acad. Sci. U.S.A.*, **69**, 115 (1972).
(24) D. B. Boyd, *J. Am. Chem. Soc.*, **91**, 1200 (1969).

Communications to the Editor

²H NMR as a Probe of the Stereochemistry of Enzyme Reactions at Prochiral Centers. Deamination of Cadaverine, Catalyzed by Diamine Oxidase

Sir:

Diamine oxidase (E.C. 1.4.3.6, diamine:oxygen oxidoreductase (deaminating)) catalyzes the oxidative deamination of a wide range of primary amines, including diamines, histamine, and arylalkylamines.[1-3] The aliphatic diamines, cadaverine and putrescine, are the substrates which are most readily oxidized. Thus, cadaverine (**2**), by loss of one of the two equivalent amino groups, yields 5-aminopentanal (**3**), which is in equilibrium with its cyclized form, Δ^1-piperideine (**4**).[4-6] It is to be expected that the reaction takes place in a sterically controlled manner. The oxidation of histamine, catalyzed by hog kidney diamine oxidase,[7] and that of benzylamine, mediated by diamine oxidase from pea seedlings,[8] takes place with stereospecific release of one of the two enantiotopic hydrogen atoms from the carbon adjacent to nitrogen. In the latter case, the stereochemistry of the reaction was determined by means of tritium labeling and determination of ^{3}H/^{14}C ratios. The chirality of the analogous oxidation of tyramine, catalyzed by monoamine oxidase (E.C. 1.4.3.4) of rat liver, was determined by a kinetic method, using deuterium labeled substrates.[9]

The stereochemistry of the oxidative deamination of cadaverine has not been established. We have employed ²H NMR spectrometry to demonstrate that, in the course of this reaction, catalyzed by diamine oxidase of hog kidney (E.C. 1.4.3.6), it is the *pro-S* hydrogen which is removed stereospecifically from the carbon atom adjacent to the reacting amino group.

The enantiomers of [1-²H]cadaverine, required for the study, were prepared by decarboxylation of L-lysine (**1**), catalyzed by L-lysine decarboxylase (E.C. 4.1.1.18, L-lysine

carboxylyase) from *Bacillus cadaveris*, a reaction which is known[10] to proceed with retention of configuration. (+)-(*S*)-[1-²H]Cadaverine dihydrochloride (**2A**) (>95% deuterated at the *pro-S* position of one of the terminal carbon atoms)[11] was obtained from the L-component of DL-[2-²H]-lysine.[12] (−)-(*R*)-[1-²H]Cadaverine dihydrochloride (**2B**) (>95% deuterated at the *pro-R* position of one of the terminal carbon atoms)[11] was obtained by decarboxylation of L-lysine in deuterium oxide (99.7 atom %, Merck Sharp and Dohme). A third deuterated cadaverine, [1,1-²H₂]cadaverine (**2C**) (>95% perdeuterated at one of the terminal C atoms),[11] was prepared by decarboxylation of DL-[2-²H]lysine in deuterium oxide.

In separate experiments, each of the three deuterated samples of cadaverine (40 mg) was incubated (37 °C, 40 h) with hog kidney diamine oxidase (Sigma Grade II, 200 mg),

Scheme I